

Iron mobilization, cytoprotection, and inhibition of cell proliferation in normal and transformed rat hepatocyte cultures by the hydroxypyridinone CP411, compared to CP20: a biological and physicochemical study

François Gaboriau^a, Karine Chantrel-Groussard^a, Nafissa Rakba^a,
Pascal Loyer^a, Nicole Padeloup^a, Robert C. Hider^b,
Pierre Brissot^a, Gérard Lescoat^{a,*}

^aInserm U 522, Equipe: “Foie, fer et autres métaux”, CHU de Rennes, Hôpital Pontchaillou, Rennes, France

^bDepartment of Pharmacy, School of Health and Life Sciences, King's College, London, UK

Received 8 September 2003; accepted 7 December 2003

Abstract

The present study analyzes the iron mobilization, the cytoprotective, and the antiproliferative effects of the lipophilic hydroxypyridinone CP411, in comparison with the hydrophilic chelator CP20 or deferiprone used in the treatment of iron overload. Primary rat hepatocyte cultures and the rat hepatoma cell line Fao were used. Chelator cell uptake was evaluated by mass spectrometry in the two models. This method was also used to investigate the stability of the chelators in an acellular system as well as their scavenging and chelating effects against the hydroxyl radical generated by the Fenton reaction. The iron mobilization and the cytoprotective effects of the chelators were evaluated in primary cultures by measuring respectively ⁵⁵Fe and lactate dehydrogenase release in the culture medium. The antiproliferative effect of the chelators was studied using the Fao cell line and measuring DNA synthesis by thymidine incorporation and DNA content by flow cytometry. We observed that CP411 entered the hepatocytes and the Fao cells respectively 4 and 13 times more than CP20. CP411 was 2.5 times more effective than CP20 to mobilize iron from preloaded hepatocytes. Pretreatment of the hepatocytes with CP20 or CP411 decreased the toxic effect of iron and CP411 was 1.6 times more effective than CP20. A dose-dependent decrease of DNA synthesis, correlated to an accumulation of cells in S phase, was observed in the Fao cell line in the presence of CP411, while CP20 was without effect. CP411 effect was inhibited by addition of iron simultaneously with the chelator, the addition of Zn or Cu was without effect. The inhibitory effect of CP411 was reversible since, 24 hr after removal of the chelator, DNA replication reached the control level. The results show that CP411 is more efficient to protect the hepatocyte from the toxic effect of iron load and to inhibit tumor cell proliferation. Its higher efficiency may result from its better cell uptake since equimolar solutions of the two chelators in an acellular system exhibit the same ability to inhibit the Fenton reaction.

© 2004 Elsevier Inc. All rights reserved.

Keywords: Hydroxypyridinone iron chelator; Hepatocyte; Cytoprotection; Antiproliferative effect

1. Introduction

As McCance and Widdowson [1] suggested from early studies, iron balance in man is essentially controlled by

absorption of dietary iron in the proximal small intestine because excretory pathways are extremely limited. As a result, a progressive accumulation of iron in the body, particularly in the liver, leads to iron overload which is toxic and can induce hepatocellular carcinoma development as observed in genetic and secondary hemochromatosis [2,3]. In addition, iron is known to be necessary for cellular proliferation and we have previously demonstrated that iron overload is associated with increased DNA synthesis and mitotic index in rat hepatocyte cultures stimulated

* Corresponding author. Tel.: +33-2-99-54-74-06;
fax: +33-2-99-54-01-37.

E-mail address: gerard.lescoat@rennes.inserm.fr (G. Lescoat).

Abbreviations: DFO, desferrioxamine; FASII, ferrous ammonium sulfate; HVA, homovanillic acid; LDH, lactate dehydrogenase; NTBI, non-transferrin bound iron; SAL, salicylic acid; UVC, ultraviolet C.

by Epidermal Growth Factor [4]. Moreover, several studies, using different models, show that iron is implicated in tumor cell growth [5,6] and the risk of developing a hepatocellular carcinoma appears to be related to the level and duration of iron overload [7,8]. This is probably why hemochromatosis is frequently complicated by a hepatocellular carcinoma.

Thus, there is a great interest in the search for new iron chelators in order to decrease iron overload in genetic and secondary hemochromatosis. Indeed, iron depletion by different iron chelators has been shown to inhibit proliferation of various cell lines and normal activated lymphocytes *in vitro* [9–11]. We have previously demonstrated that iron depletion, induced by desferrioxamine (DFO), the hydroxypyridin-4-one CP20 or *O*-trensox decreases DNA synthesis in both normal and transformed hepatocytes [12–14]. Cell cycle studies have shown that iron depletion arrests the cell cycle in different phases depending on both the cell type and the chelator [12–17]. Moreover, several authors have reported that iron chelators induce apoptosis in proliferating cells, such as activated T-lymphocytes, the promyelocytic cell line HL60, and murine lymphoma 38C13 cells [18,19]. More recently, we demonstrated that the hexadentate chelator *O*-trensox was a better inducer of apoptosis than DFO [14]. Thus, in view of these data, iron chelators have been proposed as promising antiproliferative agents in the treatment of human cancer.

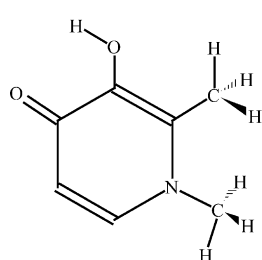
However, DFO used for the treatment of iron overload, neuroblastoma, and other diseases, such as malaria [20,21], is poorly absorbed by the gastrointestinal tract; furthermore, continuous exposure to DFO causes a dose- and time-dependent cytotoxicity [22]. Therefore, various new iron chelators have been designed for clinical use. Among them, the hydrophilic (partition coefficient = 0.17) hydroxypyridin-4-one CP20 or deferiprone (Fig. 1) has been developed as an oral iron chelator for the treatment of secondary iron overload [23–25]. In search for an alternative iron chelator to DFO, we have compared the

biological properties of several new hydroxypyridinones. We previously reported the iron mobilization and the cytoprotective effect of CP20 in normal rat hepatocyte cultures [26], and more recently an antiproliferative effect in the human hepatoblastoma cell line HepG2 [13]. The present study analyzes the iron mobilization, cytoprotective, and antiproliferative effects of the lipophilic hydroxypyridinone CP411 (Fig. 1), in comparison with the hydrophilic chelator CP20.

2. Materials and methods

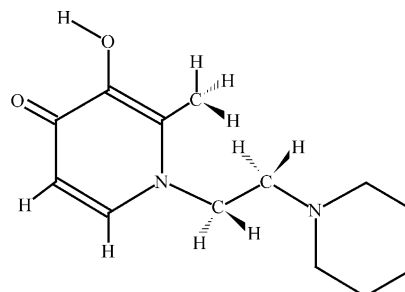
2.1. Cell cultures

Adult hepatocytes were isolated from 2-month-old male Sprague–Dawley rats (250–300 g) by perfusing the liver with a liberase solution (0.007% liberaseTM RH purified enzyme blend from Boehringer Mannheim; 0.075% CaCl₂ buffered with 0.1 M HEPES, pH 7.6 from Calbiochem) according to Seglen's method with some modifications [27,28]. Rats were maintained on a 12 hr light/dark cycle and were given diet and water *ad lib*. All procedures involving animals were done in compliance with French rules and regulations. The hepatocytes were collected in Leibovitz medium containing (per mL): glutamine (0.002 mmol), BSA (2 mg). The cell suspension was filtered through gauze and allowed to sediment for 20 min to eliminate cell debris, blood, and sinusoidal cells. The cells were then washed three times by centrifugation (100 g during 2 min), tested by Trypan blue dye exclusion for viability (always in the range of 85–95%). The hepatocytes were then suspended in a mixture of 75% Eagle's minimum essential medium and 25% medium 199 containing (per mL): fetal calf serum (0.1 mL), glutamine (0.002 mmol), penicillin (50 IU), streptomycin (50 µg), bovine insulin (5 µg), BSA (1 mg), and NaHCO₃ (2.2 mg). For the experimental procedure, hepatocytes were plated in multiwell tissue culture plates (8 × 10⁵ cells in a well area



CP20

Mw = 139
Partition coefficient = 0.17



CP411

Mw = 236
Partition coefficient = 0.96

Fig. 1. Chemical structures of the hydroxypyridinones CP20 and CP411.

of 9.6 cm²). The medium was changed 3–4 hr later and supplemented with hydrocortisone hemisuccinate (7×10^{-7} M).

The rat hepatoma cell line Fao used in this study was obtained by Deschatrette and Weiss [29] and maintained by subculture in the following medium—50% HAM F12 medium and 50% NCTC 135 medium (Eurobio)—containing (per mL): fetal calf serum (0.1 mL), glutamine (0.002 mmol), penicillin (50 IU), streptomycin (50 µg), and NaHCO₃ (2.2 mg).

For the experiments, the hepatocytes and the Fao cells were maintained in the same medium as above but deprived of fetal calf serum.

Cell cultures were maintained during 48 hr in the control condition (neither iron nor chelators present), in presence of iron alone, chelators alone, or chelators plus divalent cations.

2.2. Iron chelators

DFO (mesylate salt) was purchased from Sigma-Aldrich Chimie. The hydroxypyridinones CP20 and CP411 were synthesized and characterized as reported by Dobbin *et al.* [30].

2.3. Chemicals

Ferric ammonium citrate, FeSO₄, CuSO₄, or ZnSO₄ solutions were prepared in sterile water. The final concentration of Fe, Cu, or Zn in the stock solutions was 1 mM. These solutions were diluted in the culture medium to obtain a final medium iron, copper, or zinc concentration of 50 µM.

2.4. Stability of the chelators

The chemical and photochemical stability of the chelator solutions at 50 µM were established in the presence of 0.3% hydrogen peroxide (H₂O₂) and under ultraviolet C (UVC) irradiation in the absence or presence of 0.3% H₂O₂ (Fenton reaction). These experiments were conducted in 96-well microplates by using a UVC irradiator (Desaga) emitting light centered at 254 nm. At various times of incubation at 24°, 50 µL samples were collected. Both chelators, CP20 and CP411, were quantified by mass spectrometry analysis (positive mode) by monitoring the selective [CP20 + H]⁺ ion at $m/z = 140.1$ and the [CP411 + H]⁺ ion at $m/z = 237.1$, which were generated with an Atmospheric Pressure Chemical Ionization (APCI) source. Samples (10 µL) were directly injected in the auto-sampler of the HP1100 mass spectrometry analyzer, which was supplied with Chem-Station 1100 software (Agilent Technologies). The injection was performed into a stream of acetonitrile/water (3:1, v/v) at a flow rate of 0.5 mL/min. Scanning (scan range, 50–300 m/z) and Selected Ion Monitoring (SIM) mode data mass were obtained using the full

injection analysis (FIA) mode, without chromatographic separation. The following parameters were used: capillary voltage, +3000 V; corona current, 5 µA; drying gas flow rate, 6 L/min; drying gas temperature, 300°; vaporizer temperature, 400°; nebulizer pressure, 30 psig; fragmentor voltage, 80 V. Areas under the ionic signals at $m/z = 140.1$ (CP20) and at $m/z = 237.1$ (CP411) were integrated. Measurements were performed as triplicate.

2.5. Scavenging and chelating effects against the hydroxyl radical formation

The reactive hydroxyl radicals were generated from hydrogen peroxide by reaction with transition metals, such as iron(II), in a Fenton-type mechanism. This method permits the detection of both the protecting effect of chelators on the hydroxyl radical formation (by chelating the metal) and their scavenging action by reacting with this radical. Hydroxyl radical formation was monitored by the disappearance of salicylic acid (SAL) and by the concomitant formation of its main oxidation product resulting from the addition of one hydroxyl group (SAL + OH). We monitored the inhibiting effect of the chelators on the SAL hydroxylation.

To eliminate trace metal ions, all samples were prepared in an ultrapure Millipore water, previously filtered on a Chelex 100 ion exchanger. Hydrogen peroxide (0.3%) was added to 1 mL of SAL in water (1 mM) in the presence of various chelator concentrations (0, 50, 100, and 200 µM). Hydrogen peroxide and the chelators when tested alone were established to be inefficient at SAL hydroxylation. Hydroxyl radical formation was initiated by the addition of a 10 mM ferrous ammonium sulfate (FASII) stock solution in water (final FASII concentration 100 µM). Each 1.5 min, 10 µL samples were directly injected from the HP1100 series autosampler into a stream of acetonitrile at a flow rate of 0.5 mL/min.

Both the parent compound (SAL) and its hydroxylated product (SAL + OH) were detected by mass spectrometry analysis (negative mode) by monitoring their selective [SAL – H][–] ion at $m/z = 137$ and the [SAL + OH – H][–] ion at $m/z = 153$. At the relatively high concentration of SAL (1 mM) no low mass ions were interfering with the SAL and SAL + OH ions. These ions were generated by electrospray ionization and selectively analyzed by FIA without chromatographic separation. Scanning (scan range, 50–300 m/z) and SIM mode data mass were obtained with the following parameters: capillary voltage, –3000 V; drying gas flow rate, 6 L/min; drying gas temperature, 300°; nebulizer pressure, 30 psig; fragmentor voltage, 80 V. Kinetics of the hydroxylation reaction in the absence or presence of various chelator concentrations were deduced from the ionic intensity of the [SAL – H][–] ion at $m/z = 137$. Kinetic rate was shown to be changed less than 5% in the range of temperature 25–35°. Each kinetic determination was performed as triplicate.

2.6. Inhibition of the homovanillic acid (HVA) autoxidation

The main advantages of the HVA autoxidation assay were previously shown to be its versatility to investigate in a single run both the scavenging and inhibitory components of the antioxidant capacity, and its relevance to the reactive hydroxyl radical [31]. Autoxidation of HVA gives rise to fluorescent dimers. Their relative fluorescence intensity ($\lambda_{\text{exc}} = 315 \text{ nm}$; $\lambda_{\text{em}} = 425 \text{ nm}$) follows a linear kinetic pattern (for less than 50 min). This Fenton-like reaction was transiently stopped by various reactive oxygen species scavengers (delay) while metal chelating agents, such as DFO, EDTA, and polyamines, only reduced its rate. The final reaction mixture for the HVA assay contained $3 \times 10^{-4} \text{ M}$ HVA in 0.1 M borate buffer (pH 9.0). A final volume of $200 \mu\text{L}$ was incubated at 37° under gentle stirring in each well of a 96-well microplate. Fluorescence was measured every minute for 30 min, using a Gemini model fluorescence microplate reader (Molecular Devices). Autoxidation rate in the absence (R_0) or in the presence of various chelator concentrations (R_a) was calculated from the slope of these fluorescence kinetics. Each kinetic determination was performed as triplicate.

2.7. Chelator uptake measurement

Chelator uptake was investigated in both primary hepatocyte cultures and in the rat hepatoma cell line Fao. Three million cells were seeded in 25 cm^2 culture flasks. Cell treatments were performed as triplicate in the absence (control) or in the presence of $50 \mu\text{M}$ CP20 or CP411, a chelator concentration usually tested previously [12–14,26]. After 48 hr of treatment, the supernatants were removed and the cells were then washed three times with 3 mL of ice-cold PBS solution. They were collected by scraping them after adding 1 mL of water and sonicated for 30 s at 0° . Protein content in these cell extracts was measured by the Bradford method [32]. Ultrafiltration of $200 \mu\text{L}$ of the cell lysates was performed by centrifugation for 20 min at $15,000 g$ in NANOSEPTM 3K centrifugal device (Pall Filtron Co). Both chelators were quantified in these cell lysates by mass spectrometry as described above. No ion was observed at $m/z = 140.1$ (CP20) and $m/z = 237.1$ (CP411), in the mass spectra of the cell lysates obtained from control untreated hepatocytes. Cell lysate samples ($50 \mu\text{L}$) were directly injected from the HP1100 series autosampler into a stream of acetonitrile/water (3:1, v/v) at a flow rate of 0.5 mL/min . Areas under the ionic signals at $m/z = 140.1$ (CP20) and at $m/z = 237.1$ (CP411) were integrated using the Chem-Station 1100 software. Chelator concentrations were then deduced by using the calibration curves obtained from cell lysate enrichments with various concentrations of the two chelators followed by their sonication and ultrafiltration.

Each chelator measurement, which was determined as triplicate, was corrected from the protein content in the cell extracts.

2.8. Iron mobilization by the chelators

For the iron mobilization, hepatocytes were iron loaded by adding $20 \mu\text{M}$ iron– $0.02 \mu\text{M}$ [^{55}Fe]citrate to the culture medium during 24 hr. After iron loading, the hepatocytes were incubated with $50 \mu\text{M}$ CP20 or CP411; ^{55}Fe release was measured over a period of 24 hr. Extracellular radioactivity was expressed in percent of the total radioactivity of the culture.

2.9. Enzyme assay

Lactate dehydrogenase (LDH) activity was measured in both the culture medium and intracellularly as an index of cytotoxicity, employing LDH kits (Bayer Diagnostics) adapted to the Alcyon 300 analyzer (Alcyon). Extracellular LDH activity was measured on an aliquot of cell-free medium obtained by centrifugation of the medium ($1270 g$ during 5 min). Intracellular LDH activity was evaluated on hepatocytes previously lysed in phosphate saline buffer by sonication for 15 s and centrifuged as above. Experimental results were expressed in terms of LDH release into the medium given as a percentage of the total activity of the culture.

2.10. Cytoprotective effect of the chelators

The cytoprotective effect of the chelators was evaluated in primary rat hepatocyte cultures pretreated during 24 hr by $50 \mu\text{M}$ CP20 or CP411 and then exposed during 24 hr to $50 \mu\text{M}$ iron ammonium citrate. The LDH ratio (extracellular LDH/total LDH) of the cultures was measured as the toxicity parameter.

2.11. Antiproliferative effect of the chelators

In order to evaluate DNA synthesis, [^3H]methyl-thymidine (Amersham) was added to the culture medium at a final concentration of $1 \mu\text{Ci/mL}$ during 24 hr, before cell harvesting. DNA synthesis was evaluated by measuring [^3H]methyl-thymidine incorporation into TCA-precipitable DNA in the absence or in presence of the chelators. The total protein content of the cultures was evaluated by the method of Bradford [32]. Results were expressed as percent of control values.

Analysis of DNA content was performed by flow cytometry. After cell trypsinization, DNA content was measured in cells using cycle test Plus kit (Becton Dickinson). Cell cycle analysis was performed using FACScan flow cytometer (Becton Dickinson) equipped with an argon laser (488 nm). Data analysis was done using the Modfit software.

2.12. Statistical analysis

Results from at least four replicates were expressed as means \pm SD. Statistical analysis was performed using the non-parametric Mann–Whitney test. The significant level was set at 0.01.

3. Results

3.1. Physicochemical properties of the chelators

3.1.1. Chemical and photochemical stability

CP20 and CP411 in aqueous solutions were stable at 24° (Fig. 2) as well as for periods up to 24 hr (data not shown). Hydrogen peroxide (0.3%) did not significantly change the chelator concentration. In contrast, UVC irradiation led to the complete disappearance of CP20 in 20 min and CP411 to a lesser extent (50%). These two chelators were shown to absorb UVC light with maxima centered at 278 nm ($\epsilon = 11,600 \text{ L}\cdot\text{moles}^{-1}\cdot\text{cm}^{-1}$) and 282 nm ($\epsilon = 13,500 \text{ L}\cdot\text{moles}^{-1}\cdot\text{cm}^{-1}$) for CP20 and CP411, respectively. These chelators and more particularly the CP20 gave rise to photochemical reactions leading to their photooxidation. This photochemical unstability ruled out the possibility to test their reactivity against the hydroxyl radical produced from the UVC-induced photolysis of the hydrogen peroxide.

3.1.2. Scavenging and chelating effects against the hydroxyl radical formation

Hydroxyl radical formation mediated by transition metals, such as iron(II), is hypothesized to be an important

physiological condition, and is thought to be associated with oxidative damage *in vivo*, rather than H_2O_2 itself. When the various chelator concentrations (ranging from 0 to 200 μM) were incubated with the $\text{H}_2\text{O}_2/\text{Fe}^{2+}$ -dependent hydroxyl radical generating system, they can chelate the metal and prevent the radical formation and/or react with the hydroxyl radical. In this case, the kinetics of SAL loss depends on both their Fe^{2+} chelating efficiency and their relative reactivity against this radical (scavenging effect). As shown in Fig. 3A, in the absence of chelator, SAL was completely oxidized after 15-min incubation at 35°. CP20 and CP411 (100 μM) partly inhibits this effect. Dose–inhibition curves obtained at 15-min incubation are shown in Fig. 3B. Concentrations required to inhibit 50% of the hydroxyl-induced SAL loss (IC_{50}) have been deduced from a 4-parameter fit of these dose–effect curves. These values are 85 and 100 μM for CP20 and CP411, respectively. During the time course of these kinetics the chelator concentrations, as deduced from

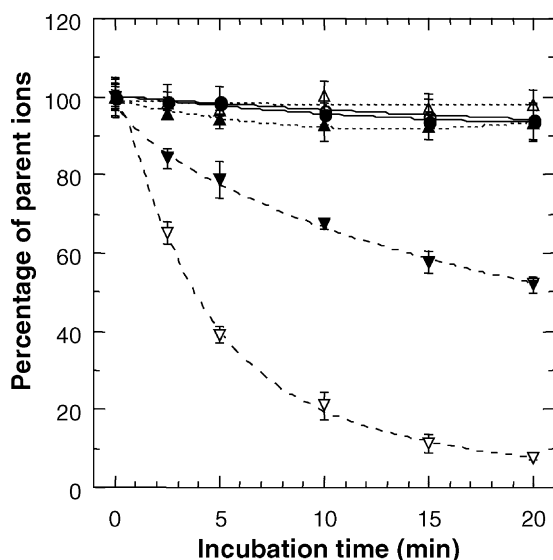


Fig. 2. Chemical and photochemical stability of the chelators in solution. Chelator solutions (50 μM) were incubated under gentle stirring at 24° (—○—, CP20; —●—, CP411), in the presence of 0.3% hydrogen peroxide (···△···, CP20; ···▲···, CP411) or under UVC exposure (—▽—, CP20; —▼—, CP411). The chelator concentrations were measured by mass spectrometry analysis.

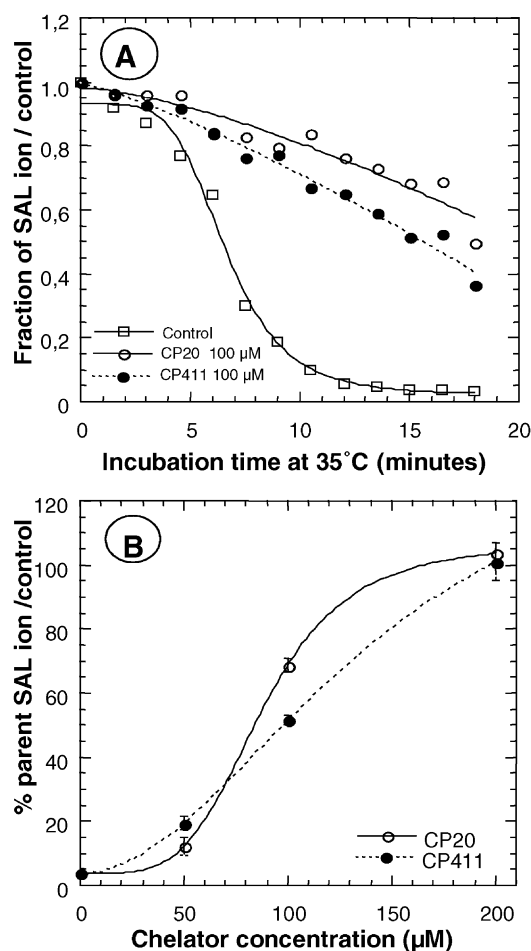


Fig. 3. Chelating efficiency of CP20 and CP411 against the hydroxyl radical generated from the Fenton reaction (hydrogen peroxide 0.3% and 100 μM FASII). (A) The kinetic of the SAL loss, monitored by mass spectrometry detection ([SAL – H] ion at m/z 137 uma), were followed at 35° in the presence of 100 μM CP20 (—○—), 100 μM CP411 (···●···), or in absence of chelator (—□—). (B) Dose–inhibition curves deduced from the fraction of salicylate ion remaining after 15-min incubation at 35° in the presence of hydrogen peroxide 0.3% and 100 μM FASII and with various concentrations of CP20 (—○—) and CP411 (···●···).

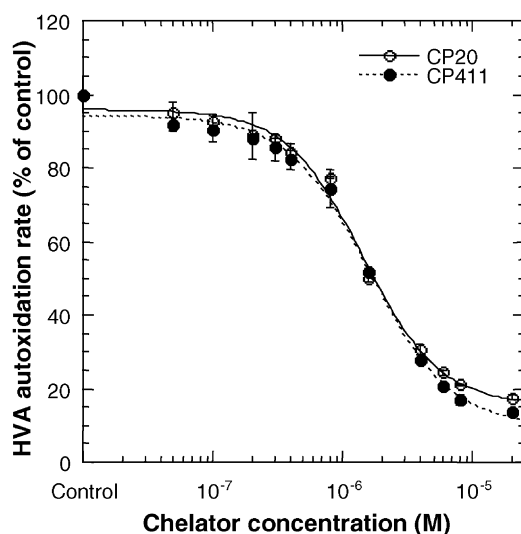


Fig. 4. Inhibition of the HVA autoxidation rate (Fenton-like reaction) by various concentrations of CP20 (—○—) and CP411 (···●···).

their mass spectrometry measurement, remain unchanged, indicating their absence of oxidative reaction with the hydroxyl radicals (data not shown).

The effect of the various chelator concentrations on HVA autoxidation rate is presented in Fig. 4. Neither was able to delay HVA autoxidation like typical scavengers (data not shown). In contrast, they were found to induce a decrease in HVA autoxidation rate. In this test, these features characterized metal chelating agents with very low scavenging properties against the reactive oxygen species which are driving HVA autoxidation (mainly hydroxyl radicals). Inhibition of HVA autoxidation rate occurred in the presence of micromolar concentrations of both chelators. Their relative efficiencies to inhibit HVA autoxidation were similar and a maximal inhibitory effect (85%) was reached at 10 μ M.

3.2. Biological effects of the chelators in primary rat hepatocyte cultures

3.2.1. Measurement of the chelator uptake by mass spectrometry

Primary rat hepatocyte cultures and Fao cells were incubated during 48 hr in the presence of 50 μ M CP20 or CP411. At the end of the incubation, the intracellular content was: 1.1 ± 0.4 nmol/mg protein and 4.6 ± 1.7 nmol/mg protein, respectively, for CP20 and CP411 in hepatocytes; 2.6 ± 0.8 nmol/mg protein and 34.1 ± 6.0 nmol/mg protein, respectively, for CP20 and CP411 in Fao cells. It appeared that CP411 entered the hepatocytes and the Fao cells respectively 4 and 13 times much more than CP20 ($P < 0.001$).

3.2.2. Iron mobilization

In the presence of chelators iron release was increased. CP411 was 2.5 times more effective than CP20; indeed,

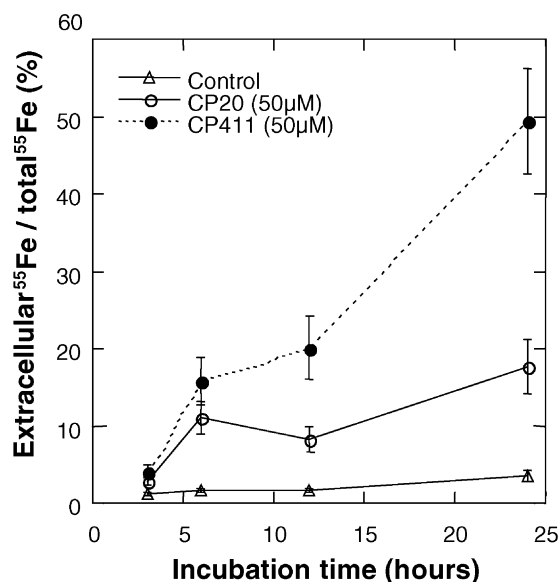


Fig. 5. Iron mobilization from rat hepatocyte cultures pretreated during 24 hr with 20 μ M iron–0.02 μ M ^{55}Fe and exposed during 3, 6, 12, or 24 hr to 50 μ M CP20 or CP411.

after 24-hr exposure to the chelators the ratio extracellular ^{55}Fe /total ^{55}Fe of the cultures was 50 and 20%, respectively, for CP411 and CP20 (Fig. 5; $P < 0.001$).

3.2.3. Cytoprotective effect

In the presence of 50 μ M of iron citrate, a 2-fold increase in the LDH ratio was observed when compared to control cultures (Fig. 6; $P < 0.001$). Pretreatment of the cultures

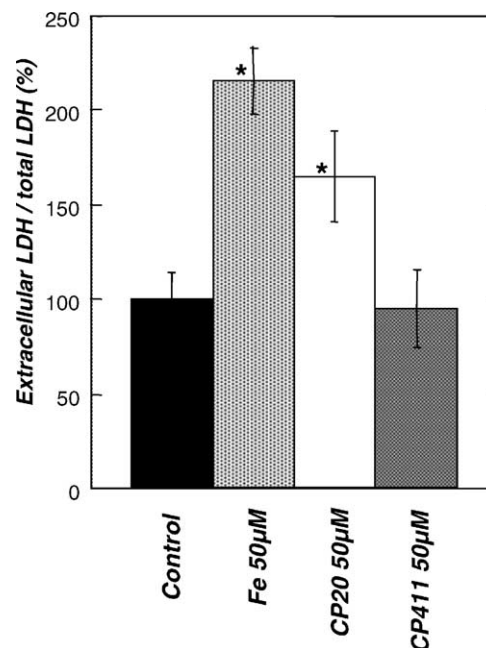


Fig. 6. Cytoprotection in rat hepatocyte cultures by CP20 or CP411. The cultures were pretreated by 50 μ M CP20 or CP411 during 24 hr; the day after only 50 μ M iron was added. The LDH ratio (extracellular LDH/total LDH) of the cultures was measured as the toxicity parameter (*significantly different from control according to the non-parametric Mann–Whitney test with $P \leq 0.01$).

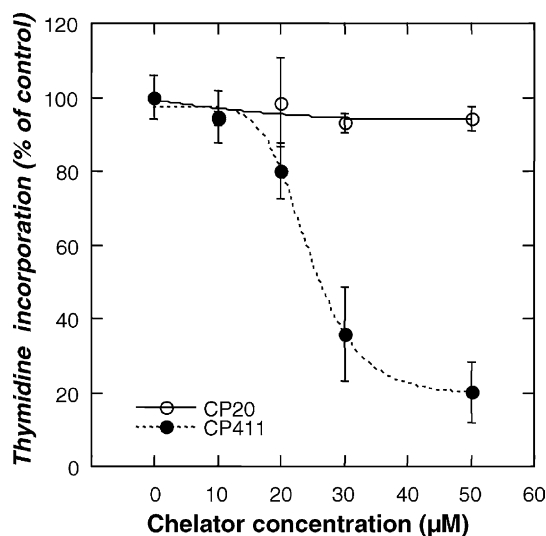


Fig. 7. Effect of increasing concentrations of CP20 or CP411 on thymidine incorporation, after 48 hr of incubation, into the rat hepatoma cell line Fao.

with 50 μM CP411 or CP20 decreased the toxic effect of iron and CP411 was more effective than CP20. Indeed, in the pretreated cultures exposed to iron citrate, the LDH ratio was similar to control for CP411 and increased by a factor of 1.6 for CP20 (Fig. 6; $P < 0.001$).

3.2.4. Antiproliferative effects of the chelators in the rat hepatoma Fao cell line

A dose-dependent decrease of DNA synthesis was observed in the presence of increasing concentrations of CP411 (0–50 μM), while comparable concentrations of CP20 were without effect (Fig. 7; $P < 0.001$ for 50 μM CP411). To further analyze the antiproliferative effect of the chelators, we measured the DNA content of Fao cells

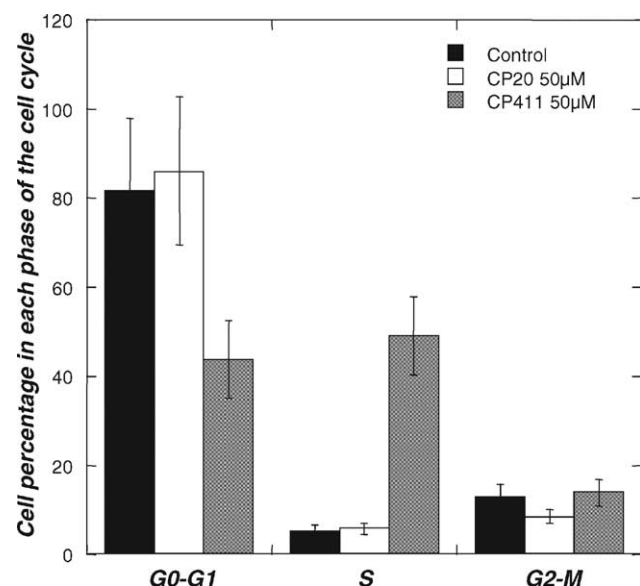


Fig. 8. DNA content analysis measured by flow cytometry in Fao cell cultures maintained 48 hr in the control condition or in the presence of 50 μM CP20 or CP411.

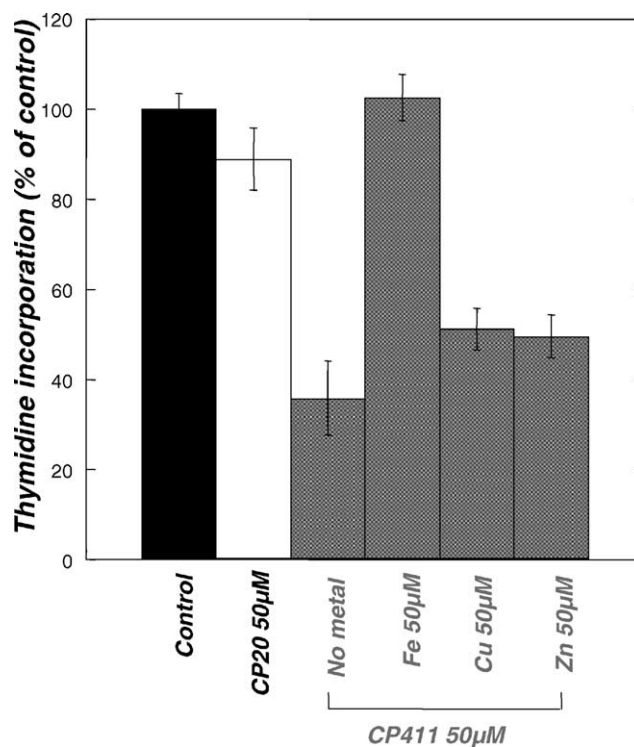


Fig. 9. Effect of addition of 50 μM iron, copper, or zinc simultaneously with 50 μM CP411 on thymidine incorporation in the rat hepatoma cell line Fao.

treated with CP20 or CP411 by flow cytometry. Compared to control cultures, CP20 was without effect on the cell percentages of the different cell cycle phases (Fig. 8). However, in the presence of CP411, the cell number was significantly decreased in G0–G1 phase (44.05% vs. 82.18%; $P < 0.001$) and increased in S phase (43.29% vs. 5.37%; $P < 0.001$).

The addition of 50 μM iron simultaneously with 50 μM CP411 inhibited the antiproliferative effect of CP411 (Fig. 9; $P < 0.001$). The addition of 50 μM copper or zinc, in the same conditions, was without effect (Fig. 9).

The inhibition of DNA synthesis by CP411 is reversible. Indeed, 24 hr after removal of the chelator from the culture medium, DNA synthesis reached the control level (data not shown).

4. Discussion

In some pathological conditions, such as iron overload diseases, iron which is usually bound to transferrin under physiological conditions, is found in plasma as non-transferrin bound iron (NTBI). NTBI exists as a range of species [33] and is assumed to play an important role in the formation of reactive oxygen species [34]. Hepatocytes are crucially important not only in general intermediary metabolism, but also in iron metabolism. In many ways, iron uptake from non-transferrin sources may prove to be extremely important in determining to what extent

parenchymal iron loading is either relatively easily handled [34–37], or leads to oxidative damage. In hemochromatosis or secondary iron overload situations, this excess iron deposition is associated with fibrosis, cirrhosis, hepatocarcinoma, arthropathy, and a dysmetabolic syndrome [38,39].

Hepatocyte cell cultures appeared to be a useful *in vitro* model system to investigate the efficiency of new iron chelators prior to their evaluation in *in vivo* models. Previous studies have used hepatocyte cultures loaded with holotransferrin [40], ferritin [41], or iron dextran [42] for the evaluation of iron chelators. In the present study, we used iron citrate which represents a possible route for introduction of iron into hepatocytes, perhaps because it is in many ways analogous to the NTBI, reported previously to be responsible for hepatic toxicity in genetic hemochromatosis [33]. Moreover, hepatocyte iron overloading with iron citrate is sustained for a long time since, 24 hr after loading the cells in the absence of chelator, only 5% of the intracellular iron is released in the culture medium. Consequently, our experimental model of iron overload, as well as the rat hepatoma cell line Fao, render it possible to compare the efficiency of different iron chelators.

For the development of iron chelators that show oral efficacy for the treatment of iron overload, attempts have been made to correlate physicochemical parameters with their biological activity. Moreover, the resulting iron–ligand complex formed should not be toxic and the coordinated iron should be protected from interaction with hydrogen peroxide or oxygen. The study of the chelator efficiency to inhibit metal-catalyzed oxidation reactions gives useful informations concerning the reactivity of the chelator–metal complexes. The two chelators CP20 and CP411 were demonstrated here to act only as metal chelators since their scavenging efficiency against the reactive hydroxyl radical generated from the Fenton reaction was demonstrated to be weak, if not null. On the basis of their ability to inhibit metal-catalyzed oxidation reaction, such as the HVA autoxidation and the SAL hydroxylation, their metal chelating capacity was assessed to be equivalent.

Some published results have already suggested that lipid solubility is also an important factor for efficiency of the chelator and its partition coefficient (K_{part}) should not be greater than one in order to allow cellular transit of the free ligand into the cell and of the complex iron–ligand out of the cell without causing cellular damage. The partition coefficient can be assessed by the distribution of the chelator between an aqueous solution and an organic solvent, e.g. water and octanol. The ability of the chelator to cross the cellular membrane is an important factor of its efficacy [43], which may be attributable to its lipophilicity [44], which would have a significant effect upon iron biliary excretion, and also to its hydrophilicity [45]. Previous results confirmed that a K_{part} close to unity appeared

to be optimal for the hydroxypyridinone efficacy for iron removal from loaded hepatocytes [30].

In the present study, the cellular chelator uptake measured by mass spectrometry, showed that CP411 entered the rat hepatocytes in primary cultures and the rat Fao hepatoma cell line cultures respectively 4 and 13 times much more than CP20. This could be related to the higher lipophilicity of CP411, which presents a partition coefficient of 8-fold higher than that of CP20. This more efficient CP411 cellular uptake could explain its higher efficiency, compared to CP20, to protect the hepatocytes from the toxic effect of iron load and to inhibit tumor cell proliferation by blocking the cell cycle at the S phase. Moreover, the cytoprotective and the antiproliferative effects of CP411 may be correlated to iron depletion since iron saturation of the chelator inhibited its biological effect, while copper or zinc were ineffective.

In conclusion, these results show that the lipophilic hydroxypyridinone CP411 enters the hepatocyte better than the hydrophilic CP20, protects the hepatocyte from the toxic effect of iron load and inhibits tumor cell proliferation with a higher efficiency than CP20. Due to its pronounced cytoprotective and antiproliferative effect, CP411 appeared to be an interesting compound for treating iron overload and for exerting an antitumoral effect.

Acknowledgments

This work was supported by the “Ligue Nationale Contre le Cancer—Conseil Scientifique Régional du Grand Ouest” and the “5^{ème} PCRDT European Contract No. QLK1-CT 2002-00444: Iron in hemochromatosis: deleterious effects of an essential nutrient”.

References

- [1] McCance RA, Widdowson EM. Absorption and excretion of iron. *Lancet* 1937;ii:680–4.
- [2] Deugnier Y, Charalambous P, Le Quilleuc D, Turlin B, Searle J, Brissot P, Powell LW, Halliday JW. Preneoplastic significance of hepatic iron-free foci in genetic hemochromatosis: a study of 185 patients. *Hepatology* 1993;18:1363–9.
- [3] Hsing AW, McLaughlin JK, Olsen JH, Møller M, Wacholder S, Fraumeni JF. Cancer risk following primary hemochromatosis: a population-based cohort study in Denmark. *Int J Cancer* 1995;60:160–2.
- [4] Chenoufi N, Lortal O, Drénou B, Cariou S, Hubert N, Leroyer P, Brissot P, Lescoat G. Iron may induce DNA synthesis and repair in rat hepatocytes stimulated by EGF/pyruvate. *J Hepatol* 1995;26:650–8.
- [5] Hann HWL, Stahlhut MW, Blumberg BS. Iron nutrition and tumor growth: decreased tumor growth in iron deficient mice. *Cancer Res* 1988;48:4168–70.
- [6] Thompson HJ, Kennedy K, Witt M, Juzefyk J. Effect of dietary iron deficiency or excess on the induction of mammary carcinogenesis by 1-methyl-1-nitrosourea. *Carcinogenesis* 1991;12:111–4.
- [7] Tarao K, Shimizu A, Ohkawa S, Harada M, Ito Y, Tamai S, Kuni Y, Okamoto N, Inoue T, Kanisawa M. Development of hepatocellular carcinoma associated with increases in DNA synthesis in the surrounding cirrhosis. *Gastroenterology* 1992;103:595–600.

- [8] Ballardini G, Groff P, Zoli M, Bianchi G, Giostra F, Francesconi R, Lenzi M, Zauli D, Cassani F, Bianchi F. Increased risk of hepatocellular carcinoma development in patients with cirrhosis and with high hepatocellular proliferation. *J Hepatol* 1994;20:218–22.
- [9] Soyano A, Chinea M, Romano EL. The effect of desferrioxamine on the proliferative response of rat lymphocytes stimulated with various mitogens in vitro. *Immunopharmacology* 1984;8:163–9.
- [10] Polson RJ, Jenkins R, Lombard M, Williams AC, Roberts S, Nouri-Aria K, Williams R, Bomford A. Mechanisms of inhibition of mononuclear cell activation by the iron-chelating agent desferrioxamine. *Immunology* 1990;71:176–81.
- [11] Richardson DR, Milnes K. The potential of iron chelators of the pyridoxal isonicotinoyl hydrazone class as effective antiproliferative agents II: the mechanism of action of ligands derived from salicylaldehyde benzoyl hydrazone and 2-hydroxy-1-naphthylaldehyde benzoyl hydrazone. *Blood* 1997;89:3025–38.
- [12] Chenoufi N, Baffet G, Drénou B, Cariou S, Desille M, Clément B, Brissot P, Lescoat G, Loréal O. Deferoxamine arrests in vitro the proliferation of porcine hepatocyte in G1 phase of the cell cycle. *Liver* 1997;18:60–7.
- [13] Chenoufi N, Drénou B, Loréal O, Pigeon C, Brissot P, Lescoat G. Antiproliferative effect of deferiprone on the HepG2 cell line. *Biochem Pharmacol* 1998;56:431–7.
- [14] Rakba N, Loyer P, Gilot D, Delcros JG, Glaize D, Baret P, Pierre JL, Brissot P, Lescoat G. Antiproliferative and apoptotic effects of *O*-Trensox, a new synthetic iron chelator, on differentiated human hepatoma cell lines. *Carcinogenesis* 2000;21:943–51.
- [15] Reddel RR, Hedley DW, Sutherland RL. Cell cycle effects of iron depletion on T-47D human breast cancer cells. *Exp Cell Res* 1985;161:277–84.
- [16] Hoyes KP, Hider RC, Porter JB. Cell cycle synchronisation and growth inhibition by 3-hydroxypyridin-4-one iron chelators in leukemia cell lines. *Cancer Res* 1992;52:4591–9.
- [17] Kulp KS, Green SL, Vulliet PR. Iron deprivation inhibits cyclin-dependent kinase activity and decreases cyclin D/CDK4 protein levels in asynchronous MDA-MB-453 human breast cancer cells. *Exp Cell Res* 1996;229:60–8.
- [18] Hileti D, Panayiotidis P, Hoffbrand AV. Iron chelators induce apoptosis in proliferating cells. *Br J Haematol* 1995;89:181–7.
- [19] Kovar J, Stunz LL, Stewart BC, Kriegerbeckova K, Ashman RF, Kemp JD. Direct evidence that iron deprivation induces apoptosis in murine lymphoma 38C13. *Pathobiology* 1997;65:61–8.
- [20] Brodie C, Siriwardana G, Lucas J, Schleicher R, Terada N, Szepesi A, Gelfand E, Seligman P. Neuroblastoma sensitivity to growth inhibition by desferrioxamine: evidence for a block in G1 phase of the cell cycle. *Cancer Res* 1993;53:3968–75.
- [21] Glickstein H, Breuer W, Loyevsky M, Konijn AM, Shanzer A, Cabantchik ZI. Differential cytotoxicity of iron chelators on malaria-infected cells versus mammalian cells. *Blood* 1996;87:4871–8.
- [22] Valle P, Timeus F, Piglion M, Rosso P, di Montezemolo LC, Crescenzo N, Marranca D, Ramenghi U. Effect of different exposures to desferrioxamine on neuroblastoma cell lines. *Pediatr Hematol Oncol* 1995;12:439–46.
- [23] Olivieri NF, Koren G, Matsui D, Liu PP, Blendis L, Cameron R, McClelland RA, Templeton DM. Reduction of tissue iron stores and normalization of serum ferritin during treatment with the oral iron chelator L1 in thalassemia intermedia. *Blood* 1992;79:2741–8.
- [24] Al-Refaie FN, Wonke B, Hoffbrand AV, Wickens DG, Nortey P, Kontoghiorghes GJ. Efficacy and possible adverse effects of the oral iron chelator 1,2-dimethyl-3-hydroxypyrid-4-one (L1) in thalassemia major. *Blood* 1992;80:593–9.
- [25] Collins AF, Fassos FF, Stobie S, Lewis N, Shaw D, Fry M, Templeton DM, McClelland RA, Koren G, Olivieri NF. Iron-balance and dose-response studies of the oral iron chelator 1,2-dimethyl-3-hydroxypyrid-4-one (L1) in iron-loaded patients with sickle cell disease. *Blood* 1994;83:2329–33.
- [26] Chenoufi N, Hubert N, Loréal O, Morel I, Padeloup N, Cillard J, Brissot P, Lescoat G. Inhibition of iron toxicity in rat and human hepatocyte cultures by the hydroxypyridin-4-ones CP20 and CP94. *J Hepatol* 1995;23:166–73.
- [27] Seglen PO. Preparation of rat liver cells. I. Effects of Ca^{2+} on enzymatic dispersion of isolated perfused liver. *Exp Cell Res* 1972;74:450–4.
- [28] Guguen C, Guillozo A, Boissard M, Le Cam A, Bourel M. Etude ultrastructurale de monocouches d'hépatocytes de rat cultivés en présence d'hémisuccinate d'hydrocortisone. *Gastroenterol Biol* 1975;8:223–31.
- [29] Deschatrette J, Weiss MC. Characterization of differentiated clones from a rat hepatoma. *Biochimie* 1974;56:1603–11.
- [30] Dobbin PS, Hider RC, Hall AD, Taylor PD, Sarpong P, Porter JB, Xiao G, van der Helm D. Synthesis, physicochemical properties and biological evaluation of *N*-substituted 2-alkyl-4(1*H*)-pyridinones: orally active iron chelators with clinical potential. *J Med Chem* 1993;36:2448–58.
- [31] Gaboriau F, Delcros JG, Moulinoux JP. A simple assay for the measurement of plasma antioxidant status using spontaneous auto-oxidation of homovanillic acid. *J Pharmacol Toxicol* 2002;47:33–43.
- [32] Bradford MM. A rapid and sensitive method for the quantitation of microgram quantities of protein utilizing the principle of protein-dye binding. *Anal Biochem* 1976;72:248–54.
- [33] Hider RC. Nature of nontransferrin-bound iron. *Eur J Clin Invest* 2002;32:50–4.
- [34] Halliwell B, Gutteridge JM. Oxygen free radicals and iron in relation to biology and medicine: some problems and concepts. *Arch Biochem Biophys* 1986;246:501–14.
- [35] De Silva DM, Askwith CC, Kaplan J. Molecular mechanisms of iron uptake in eukaryotes. *Physiol Rev* 1996;76:31–47.
- [36] Brissot P, Wright TL, Ma WL, Weisiger R. Efficient clearance of non-transferrin-bound iron by rat liver. Implications for hepatic iron loading in iron overload states. *J Clin Invest* 1985;76:1463–70.
- [37] Wright TL, Brissot P, Ma WL, Weisiger RA. Characterisation of non-transferrin-bound iron clearance by rat liver. *J Biol Chem* 1986;261:10909–14.
- [38] Deugnier Y, Guyader D, Crantok L, Lopez JM, Turlin B, Yaouanq J, Jouanolle H, Campion JP, Launois B, Halliday JW, Powell LW, Brissot P. Primary liver cancer in genetic hemochromatosis: a clinical, pathological and pathogenetic study of 54 cases. *Gastroenterology* 1993;1104:228–34.
- [39] Turlin B, Deugnier Y. Iron overload disorders. *Clin Liver Dis* 2002;6:481–96.
- [40] Baker E, Wong A, Peter H, Jacobs A. Desferrithiocin is an effective iron chelator in vitro and in vivo but ferrithiocin is toxic. *Br J Haematol* 1992;81:424–31.
- [41] Rakba N, Aouad F, Henry C, Caris C, Morel I, Baret P, Pierre JL, Brissot P, Ward RJ, Lescoat G, Crichton R. Iron mobilisation and cellular protection by a new synthetic chelator *O*-Trensox. *Biochem Pharmacol* 1998;55:1797–806.
- [42] Henry C, Rakba N, Imbert D, Thomas F, Baret P, Serratrice G, Gaude D, Pierre JL, Ward RJ, Crichton RR, Lescoat G. New 8-hydroxyquinoline and catecholate iron chelators: influence of their partition coefficient on their biological activity. *Biochem Pharmacol* 2001;62:1355–62.
- [43] Porter JB, Gyparakis M, Burke L, Huehns ER, Sarpong P, Saez V, Hider RC. Iron mobilization from hepatocyte monolayer cultures by chelators: the importance of membrane permeability and the iron-binding constant. *Blood* 1988;72:1497–503.
- [44] Zanninelli G, Glickstein H, Breuer W, Milgram P, Brissot P, Hider RC, Konijn AM, Libman J, Shanzer A, Cabantchik ZI. Chelation and mobilization of cellular iron by different classes of chelators. *Mol Pharmacol* 1997;51:842–52.
- [45] Meyer-Brunot HG, Keberle H. Biliary excretion of ferrioxamines of varying liposolubility in perfused rat liver. *Am J Physiol* 1968;214:1193–200.